SCATTERED LIGHT SIGNATURES OF MAGNETIC ACCRETION IN CLASSICAL T TAURI STARS

KENNETH WOOD[1] AND BARBARA WHITNEY[2]

ABSTRACT

The magnetic accretion model as applied to T Tauri stars predicts the formation of hot spots or rings on the stellar surface where accreting disk material impacts the stellar surface at or near the magnetic poles. When the magnetic poles are not aligned with the stellar rotation axis, or the hot spots are nonuniform, brightness variations arise as the hot spots rotate into and out of view. We have investigated the effects on the scattered light images of a T Tauri star-plus-disk system of nonaxisymmetric illumination of the circumstellar disk by hot starspots. We find that changes in the scattered light pattern occur during a stellar rotation period. These changes are observable with current high-resolution imagery and provide a further observational test of the magnetic accretion theory. The observed brightening and dimming of HH 30's scattered light disk may be explained by such a model, although further synoptic observations are required to confirm this.

Subject headings: accretion, accretion disks — stars: pre–main-sequence — stars: rotation — stars: spots

1. INTRODUCTION

Photometric variability is a ubiquitous characteristic of T Tauri stars, and *periodic* photometric variability has now been confirmed in hundreds of systems (e.g., Bouvier et al. 1993; Wichmann et al. 1998; Choi & Herbst 1996; Makidon et al. 1997). A favored explanation for such periodic variability is stellar spots. Cool spots have been mapped through Doppler imaging of weak-lined T Tauri stars (e.g., Hatzes 1995), while hot spots tend to be associated with (often stochastic) variability in classical T Tauri stars: the star-plus-disk systems (e.g., Kenyon et al. 1994; Bouvier et al. 1993; Eaton, Herbst, & Hillenbrand 1995; Choi & Herbst 1996; Herbst et al. 1994). In classical T Tauri stars, the photometric variability is thought to be associated with the accretion process, and the currently favored magnetic accretion models naturally provide a source of variability.

The magnetic accretion model (Ghosh & Lamb 1979a, 1979b; Königl 1991; Shu et al. 1994; Ostriker & Shu 1995; Najita 1995) as applied to T Tauri stars is characterized by (1) a star surrounded by a geometrically thin, optically thick, circumstellar disk that is truncated within a certain inner radius, (2) a stellar dipole magnetic field that threads the disk and (3) accretion "streams" of disk material that flow along field lines and impact the star at the magnetic poles, producing hot spots (or "rings;" Mahdavi & Kenyon 1998). The presence of hot spots or rings on the stellar surface has observable consequences. Periodic photometric variations will be produced as the star's rotation brings the spots into and out of view; periodic polarimetric variations have also been predicted (e.g., Gullbring & Gahm 1996) due to periodically varying illumination of the disk by the spots. We have investigated the photopolarimetric variability produced by such a theory (Wood et al. 1996; Stassun & Wood 1998) where the hot accretion region was modeled as spots or rings on the stellar surface, and the polarization arises from the scattering of stellar and hot-spot radiation in the disk. Strictly periodic correlated modulations of the photometry and polarimetry are obtained when the accretion rate is constant throughout a stellar rotation period. With a variable

accretion rate, we found that the photopolarimetry was stochastic (as expected) but that the same correlation between photometry and polarimetry existed—maximum polarization at minimum brightness, as observed in several sources (e.g., Drissen, Bastien, & Louis 1989).

Motivated by the numerous observations of photometric variability, in this Letter we make predictions of the variability that may be observed in high-resolution scattered light images of classical T Tauri stars. Indeed, recent *Hubble Space Telescope* observations of HH 30's edge-on disk (Burrows et al. 1996) showed that the scattered light nebula changed in brightness between the two observations. We have constructed a model that comprises a flared disk with the same mass and structure determined for HH 30 (Burrows et al. 1996; Wood et al. 1998) and nonaxisymmetric illumination by diametrically opposed hot spots on the stellar surface. The nonaxisymmetric illumination of the circumstellar disk by the starspots leads to observable differences in the scattered light images throughout the stellar rotation period, and for almost edge-on viewing (appropriate to HH 30) the brightness variations are in agreement with those observed. In the following sections, we present the geometry employed in the simulations, the resulting scattered light images, and conclude with a summary of these results as they apply to HH 30.

2. MODEL PARAMETERS AND RADIATION TRANSFER TECHNIQUE

The model comprises a central spherical star of temperature 3800 K (appropriate for the suspected M 0 spectral type of HH 30; Kenyon et al. 1998), with two diametrically opposed circular spots of temperature 10,000 K with radii 20°, located at latitudes $\pm 65°$. The spots cover 6% of each hemisphere. This spotted star is surrounded by a flared circumstellar disk with inner and outer radii 3 $R_\star$ and 250 AU. The dust plus gas in the disk is distributed with the standard geometry as prescribed by Shakura & Sunyaev (1973),

$$\rho = \rho_0 \exp\left\{ -\frac{1}{2}\,[z/h(\varpi)]^2 \right\} \Big/ \varpi^\alpha, \qquad (1)$$

where ϖ is the radial coordinate in the disk midplane and the

[1] Smithsonian Astrophysical Observatory, 60 Garden Street, Cambridge, MA 02138; kenny@claymore.harvard.edu.
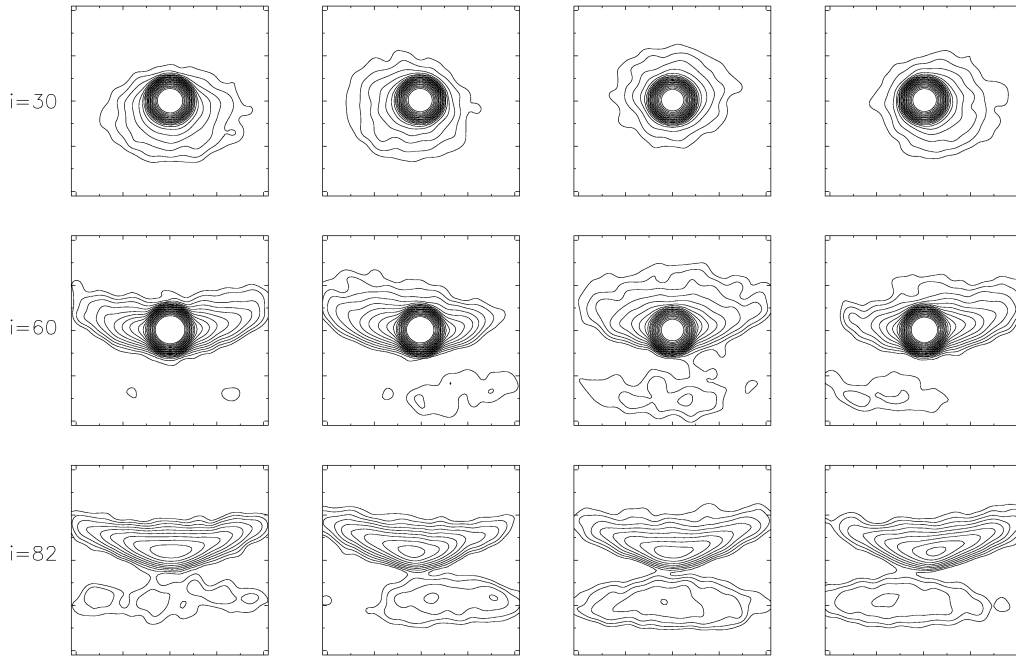[2] Prism Computational Sciences Inc., 16 North Carroll Street, Suite 950, Madison, WI 53703; whitney@prism-cs.com.

FIG. 1.—*I*-band scattered light models for the spotted star-plus-disk system described in the text. The three rows are for system inclinations of 30°, 60°, and 82°, and the four columns are for rotational phases of 0°, 90°, 180°, and 270°. The contour levels are spaced at half-magnitude intervals with the lowest contour being at 3×10^{-5} of the peak value for the 30° and 60° cases and at 0.03 of the peak value for the 82° case. The images have been convolved with a Gaussian point-spread function with a FWHM of 30 AU. Each image is 420 AU on a side, and the star is rotating clockwise as viewed from the 30° row. In the first and third panels, the spot on the upper hemisphere is at azimuths of 0° and 180°, respectively—i.e., bottom and top of these panels for the 30° row. Notice how the scattered light pattern changes at all viewing angles as the bright spots illuminate different regions of the disk. For the 82° row, the brightening and dimming of the upper and lower nebulae is close to that observed in HH 30.

scale height increases with radius according to

$$ h = h_0 \left(\frac{\varpi}{R_\star} \right)^\beta . \qquad (2) $$

Following Burrows et al. (1996) and Wood et al. (1998), we adopt the following parameters appropriate to HH 30's disk: $\beta = 9/8$, $\alpha = 15/8$, $h_0 = 0.05 R_\star$ (giving $h[100 \text{ AU}] = 15$ AU), and a disk mass of $2.5 \times 10^{-4}\ M_\odot$.

The radiation transfer is performed with the Monte Carlo technique (Whitney & Hartmann 1992; Wood et al. 1996, 1998; Stassun & Wood 1998). For the 100 AU size scales associated with T Tauri disks, the light-travel times are on the order of a day. Since the observed rotation periods of classical T Tauri stars are of the order of several days to weeks with the peak of the distribution occurring around 7 or 8 days (Attridge & Herbst 1992; Bouvier et al. 1993; Edwards et al. 1993; Eaton et al. 1995), we have not included the light-travel time effects on the illumination of the disk in our calculations. The simulations are performed at the *I* band where we assume the dust plus gas mixture in the disk has the same properties as the Kim, Martin, & Hendry (1994) mixture: albedo $a = 0.5$, scattering asymmetry parameter $g = 0.4$, and total opacity $\kappa = 105\ \text{cm}^2\ \text{g}^{-1}$.

3. SCATTERED LIGHT IMAGES

Figure 1 shows the resulting *I*-band scattered light images at four different rotational phases. The three sets of figures are for system inclinations of 30° and 60° where the central star is revealed and the more edge-on viewing angle of 82° appropriate for HH 30's disk. Figure 2 shows the *I*-band light curves for the entire stellar rotation period, with the squares marking the phases of the images. We have scaled these light curves

so that for the 82° case, $I \approx 17$, which has been measured for HH 30 (Mundt & Fried 1983). For the lower inclinations, Figure 2 shows that the source will appear more than 5 mag brighter since the star is seen directly and not obscured by the disk. Low inclinations show less photometric variability (0.5 mag) since the upper hot spot is visible throughout the stellar
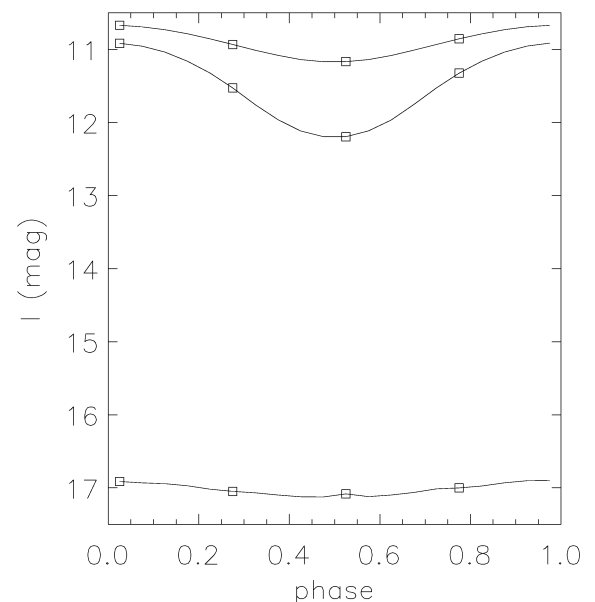

FIG. 2.—*I*-band light curves for the model system. The squares show the rotational phases where the images in Fig. 1 are plotted. The upper curve is for the 30° inclination, the middle is for 60°, and the lower is for the 82° case. Note that the 82° case is more than 5 mag fainter than the inclinations where the central star is revealed.

rotation. At intermediate inclinations when the hot spot is oc-culted by the star, large photometric variability occurs, as seen in the 1.5 mag variation in the 60° case in Figure 2. For edge-on viewing the disk obscures the star, but changes in the scat-tered light as the spots illuminate different regions of the disk result in a variation of about 0.2 mag for this particular star-spot-disk system. This light curve shows a secondary maximum around rotational phase 0.5, where we see scattered light from the upper surface and also from the lower surface, which is illuminated by the spot on the lower hemisphere (see Stassun & Wood 1998 for a more thorough investigation of the pho-topolarimetric variability). Although in Figure 1 the scattered flux for lower inclinations is at levels typically 10^{-4} of the peak flux per pixel (where our model pixels are 5 AU on a side), recent observations of GM Aur have detected scattered light from a disk in just such a system ($i \approx 60°$) with point-spread function subtraction from Wide Field Planetary Camera 2 im-ages (Stapelfeldt et al. 1995). Therefore, the variations in our simulations should be detectable for these low-inclination sys-tems. The scattered light pattern clearly changes as the star and the illuminating hot spots light up different regions of the disk. Since the disk is very optically thick, at the lowest inclination the effect of the second spot is not seen, and the changes in image morphology arise from disk illumination by the spot on the upper hemisphere. For the 60° simulation, low levels of scattered light from the lower half of the disk are detected (see also Whitney & Hartmann 1992).

The lower four panels of Figure 1 show the changes in the scattered light morphology of a nearly edge-on system where the central star is obscured by the dense equatorial regions of the disk. The lower portion of the nebula (the side that is further from the observer) gets brighter between the first and third panels. This is because in the first panel the geometry is such that the spot on the lower hemisphere is at a stellar longitude of 180° and light from it cannot illuminate the lower parts of the disk observable to us. The upper spot is at longitude 0°, and its light illuminates the upper half of the disk that we see. In the third panel, the illuminating geometry is reversed and the lower nebula has brightened and the upper dimmed. The upper nebula is always brighter because of the disk inclination (Whitney & Hartmann 1992). The first and third panels show axisymmetric scattered light nebulae, but the second and fourth panels show a nonaxisymmetric image resulting from the il-luminating spots lying close to the stellar limb. Thus a further prediction of the magnetic accretion model, testable with high-resolution imagery, is that for edge-on disk systems the upper

and lower nebulae will brighten asymmetrically during the stel-lar rotation.

Between the first and third panel of the 82° simulation, the lower nebula brightened by 0.6 mag and the upper dimmed by 0.4 mag. These amplitudes are close to the observed variations of 0.81 and 0.46 mag for the corresponding nebulae in HH 30 (Burrows et al. 1996). The combination of HH 30's strong jet, scattered light disk, and remnant envelope (which Wood et al. 1998 found was required to fit the scattered light at high lat-itudes) suggest that accretion is ongoing in HH 30. Therefore, in view of our simulations, the observed changes may indeed be signatures of variable illumination by accretion hot spots. Further synoptic observations in imaging, photometry, and po-larimetry are needed to confirm this.

An important point to note is that when modeling scattered light images, it is essential to know the scattering geometry and illumination before attributing any observed features to dust parameters. When modeling the scattered light structures at a single epoch for HH 30 (Burrows et al. 1996) and the circumbinary disks in GG Tau and UY Aur (Close et al. 1998), these investigators varied the dust parameters until a satisfac-tory fit to the images was achieved. They adopted axisymmetric disks illuminated by central point sources. The simulations shown in Figure 1 clearly demonstrate that very different-look-ing images can arise as a result of changing illumination and unless images at different epochs are modeled, it is not possible to undertake an accurate investigation into the scattering prop-erties of the disk.

In conclusion, we have shown that changes in the mor-phology of scattered light images of classical T Tauri stars provide a further observational test of the magnetic accretion model. The brightness changes in our simulations resemble those observed in HH 30, and we propose that the observed dimming and brightening of the upper and lower nebulae of HH 30's disk as seen by *HST* may be a result of variable illumination by hot starspots. Although variations in the ac-cretion rate will not produce strictly periodic modulations (as in our simulations), a variable accretion rate (resulting in the spots possibly changing in size and temperature) will still yield correlations between the photometry, polarimetry, and image morphology.

REFERENCES

Attridge, J. M., & Herbst, W. 1992, ApJ, 398, L61
Bouvier, J., Cabrit, S., Fernandez, M., Martin, E. L., & Matthews, J. M. 1993, A&A, 61, 737
Burrows, C. J., et al. 1996, ApJ, 473, 437
Choi, P. I., & Herbst, W. 1996, AJ, 111, 283
Close, L. M., et al. 1998, ApJ, 499, 883
Drissen, L., Bastien, P., & St. Louis, N. 1989, AJ, 97, 814
Eaton, N. L., Herbst, W., & Hillenbrand, L. A. 1995, AJ, 110, 1735
Edwards, S., et al. 1993, AJ, 106, 372
Ghosh, P., & Lamb, F. K. 1979a, ApJ, 232, 259
———. 1979b, ApJ, 234, 296
Gullbring, E., & Gahm, G. F. 1996, A&A, 308, 821
Hatzes, A. P. 1995, ApJ, 451, 784
Herbst, W., Herbst, D. K., Grossman, E. J., & Weinstein, D. 1994, AJ, 108, 1906
Kenyon, S. J., Brown, D. I., Tout, C. A., & Berlind, P. 1998, AJ, 115, 2491
Kenyon, S. J., et al. 1994, AJ, 107, 2153
Kim, S. H., Martin, P. G., & Hendry, P. D. 1994, ApJ, 422, 164

König, A. 1991, ApJ, 370, L39
Mahdavi, A., & Kenyon, S. J. 1998, ApJ, 497, 342
Makidon, R. B., Strom, S. E., Tingley, B., Adams, M. T., Hillenbrand, L., Hartmann, L., Calvet, N., & Jones, B. F. 1997, BAAS, 191, 5.06
Mundt, R., & Fried, J. W. 1983, ApJ, 274, L83
Najita, J. 1995, Rev. Mexicana Astron. Astrofis., 1, 293
Ostriker, E. C., & Shu, F. H. 1995, ApJ, 447, 813
Shakura, N. I., & Sunyaev, R. A. 1973, A&A, 24, 337
Shu, F. H., Najita, J., Ostriker, E. C., Wilkin, F., Ruden, S., & Lizano, S. 1994, ApJ, 429, 781
Stapelfeldt, K., et al. 1995, BAAS, 187, 113.04
Stassun, K., & Wood, K. 1998, ApJ, in press
Whitney, B. A., & Hartmann, L. 1992, ApJ, 395, 529
Wichmann, R., Bouvier, J., Allain, S., & Krautter, J. 1998, A&A, 330, 521
Wood, K., Kenyon, S. J., Whitney, B. A., & Bjorkman, J. E. 1996, ApJ, 458, L79
Wood, K., Kenyon, S. J., Whitney, B. A., & Turnbull, M. 1998, ApJ, 497, 404